On Leaved Dipole Rose Spherical, Cylindrical and Torus Graphs

Qays R. Shakir

***Abstract*—This article presents inductive constructions for leaved dipole rose graphs that are embedded in the sphere, cylinder and torus. Specifically, for each of these three classes of surface graphs, we give a topological inductive construction which consists of a set of topological operations and a set of minimal graphs.**

***Index Terms*—sparse graph, tight graph, inductive operation, minimal graph.**

I. Introduction and Preliminaries

Consider a class of graphs, $\mathcal{G}$. One way to study and investigate specific properties of $\mathcal{G}$ is to examine an inductive construction for $\mathcal{G}$. An inductive construction of $\mathcal{G}$ is a combination of two components; a set of inductive operations and a set of small graphs in $\mathcal{G}$, which we call them here minimal. It is possible to construct each graph in $\mathcal{G}$ by conducting a sequence of some operations of the selected set of inductive operations on some minimal graphs of $\mathcal{G}$.

Selecting the minimal graphs depends on the set of inductive operations. Generally, a graph is minimal if it is not possible to perform the inverse of any inductive operation so that the result graph still remain in the same class. In the current article, we construct inductive constructions for leaved dipole rose graphs that are embedded in some surfaces of low genus.

The main purpose of initiating Inductive constructions is to build various types of graphs. For example, in [1] and [2], independent inductive constructions were presented for an interested class of graphs called Laman graphs. Other inductive constructions for specific kinds of sparse graphs can be found in [3]. Many other inductive constructions not concern with sparse can be found in the literature, [4] and [5].

For classes of graphs that are embedded in surfaces, various topological inductive constructions were initiated. Typical examples of such constructions have been created for triangulating surfaces. The key point in generating triangulations on a surface is to present a set of minimal triangulations. The natural inductive operation in that sequel is the vertex splitting and its inverse edge contraction. Usually, such triangulations are called minimal. Many studies have been carried on to find such minimal triangulations on various surfaces such as these in [6], [7] and [8]. A related problem is to investigate the existing of finite number of triangulations on surfaces was carried in [9]. There are many other studies which presented various inductive constructions on different kinds of graphs embedded in various surfaces. Interested readers are referred to the following examples of studies; [10], [11] and [12].

Manuscript received September 3, 2022; revised February 24, 2023

Qays R. Shakir is a lecturer at department of information technology, Technical College of Management-Baghdad, Middle Technical University, Iraq, (email: qays.shakir@mtu.edu.iq).

The remainder of this section is devoted to presenting some basic concepts that we use in this article. A *graph* is a pair $\Gamma = (V_\Gamma, E_\Gamma)$ where V_Γ and E_Γ is the vertex and edge sets of Γ, respectively.

An *n-leaved dipole rose* graph, L_n, is a multigraph with $n+1$ vertices and $2n$ edges with a vertex of degree $2n$, called core vertex. This graph can be constructed from a star S_n by replacing each edge in S_n by a 2-cycle. Figure 1 presents some examples of such graphs where Figure 1(a), (b), (c) and (d) is a 2, 3, 4 and 6-leaved dipole rose graph, respectively. For convenient, L_0 stands for a leaved dipole rose graph with a single vertex. The main goal of this article is to construct some classes of leaved dipole rose graphs that are embedded in some surfaces of low genus.

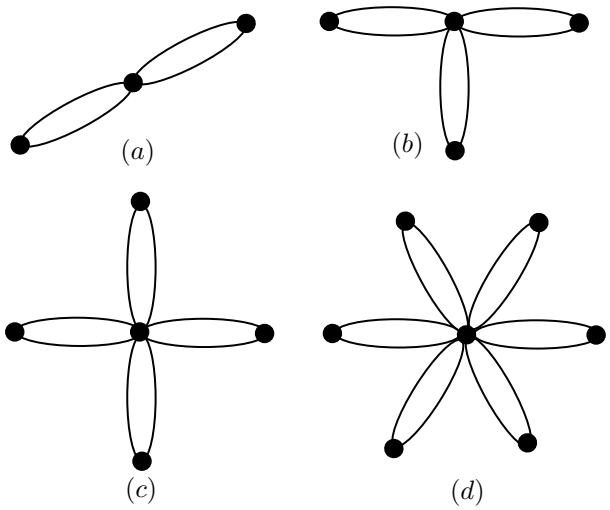

Fig. 1. Some kinds of leaved rose graphs.

Given an oriented surface $\mathcal{S}$ of a specific genus, a *surface graph* is an embedding of an abstract graph in the surface without edge crossings. An embedding of a graph Γ in $\mathcal{S}$ is a continuous 1-1 function from a topological representation of the graph Γ into $\mathcal{S}$, see [13], [14] and [15]. We use the notation $\Gamma^{\mathcal{S}}$ to indicate that this graph is a surface graph where Γ is embedded in a surface $\mathcal{S}$. A *face* of $\Gamma^{\mathcal{S}}$ is a connected component of the complement of the embedding of Γ, in the surface $\mathcal{S}$. Let r_i be the number of faces with i edges in the boundary. A face in $\Gamma^{\mathcal{S}}$ is *cellular* if it is homeomorphic to an open disc. $\Gamma^{\mathcal{S}}$ is cellular if all of its faces are cellular. Let $F_{\Gamma^{\mathcal{S}}}$ denotes the set of all faces of the cellular surface graph $\Gamma^{\mathcal{S}}$. Let F be a face of a surface subgraph H of $\Gamma^{\mathcal{S}}$. We define $int_{\Gamma^{\mathcal{S}}}(F)$ to be the surface subgraph of $\Gamma^{\mathcal{S}}$ corresponding to the vertices and edges of Γ whose images lie in the topological closure of F. Similarly, we define $ext_{\Gamma^{\mathcal{S}}}(F)$ to be the surface subgraph

of $\Gamma^{\mathcal{S}}$ corresponding to those vertices and edges of Γ whose images lie in $\mathcal{S} - F$. The *boundary* of F can be defined as $\partial F = int_{\Gamma^{\mathcal{S}}}(F) \cap ext_{\Gamma^{\mathcal{S}}}(F)$. Figure 2 shows a surface graph $\Gamma^{\mathcal{S}}$ which has a surface subgraph that is bold. The surface subgraph has a hexagon face F. The surface subgraph $int_{\Gamma^{\mathcal{S}}}(F)$ is the dark gray shaded area together with its boundary, ∂F. The surface subgraph in the light gray shaded area together with ∂F is $ext_{\Gamma^{\mathcal{S}}}(F)$.

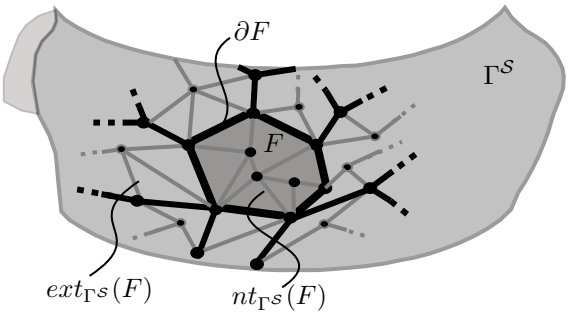

Fig. 2. A surface graph with two special subgraphs.

A loop α is *nonseparating* in $\mathcal{S}$ if the complement of the image of α has the same number of components as $\mathcal{S}$. Let α be a *nonseparating* loop in $\mathcal{S}$. Suppose that $\mathcal{S}$ has genus g and α is a nonseparating loop in $\mathcal{S}$ and α is contained within some face F of Γ^S. By cutting $\mathcal{S}$ along α and filling in the two resulting boundary curves with open discs, a new surface graph $\widetilde{\Gamma^{\mathcal{S}}}$ is obtained. The new resulting surface is of genus $g-1$. A loop α in a surface $\mathcal{S}$ is called *essential* if it is not null homotopic and otherwise α is called *inessential*, [16]. A separating and nonseparating, respectively, cycle c in a surface graph $\Gamma^{\mathcal{S}}$ is a simple closed walk whose associated simple loop is separating and nonseparating, respectively, in $\mathcal{S}$.

The main purpose of this work is to build some classes of surface graphs. Specifically, we are interested in building L^S, L^C and L^T where S, C and T stands for the sphere, cylinder and torus, receptively. To achieve this purpose, we use inductive constructions to build the interest classes of surface graphs. Hence, we need to specify the topological inductive operations for each of such classes. In the following, we define such operations in some details. Let e be an edge in Γ, then Γ/e represents a graph that is obtained from Γ by contracting an edge e and identifying its end-vertices. Let $\Gamma - e$ represents a graph that is obtained from Γ by deleting an edge e. The inductive operations that we use to construct the three classes of surface graphs are topological operations. We mainly use two topological inductive operations, namely digon and quadrilateral splitting. However, we also deal with their inverses, i.e. contraction operations, to recognise the desired minimal surface graphs. We briefly describe the two contraction operations. Consider $\Gamma^{\mathcal{S}}$ and let D be a digon in $\Gamma^{\mathcal{S}}$ with boundary walk v_i, e_i, v_j, f_j, v_i. Let $\Gamma^{\mathcal{S}}_D = \Gamma^{\mathcal{S}}/e_i - f_i$. We say that $\Gamma^{\mathcal{S}}_D$ is the surface graph that is obtained from $\Gamma^{\mathcal{S}}$ by a digon contraction, Figure 3(a). Now, let Q be a degenerate quadrilateral face in $\Gamma^{\mathcal{S}}$ with boundary walk $v_i, e_i, v_k, e_j, v_j, f_j, v_h, g_j, v_i$. Let $\Gamma^{\mathcal{S}}_Q = \Gamma^S/(v_i \sim v_j) - \{e_j, f_j\}$. We say that $\Gamma^{\mathcal{S}}_Q$ is the surface graph that is obtained from $\Gamma^{\mathcal{S}}$ by a quadrilateral contraction, Figure 3(b).

Proposition 1.1: There is no face of odd degree in $L^{\mathcal{S}}$.

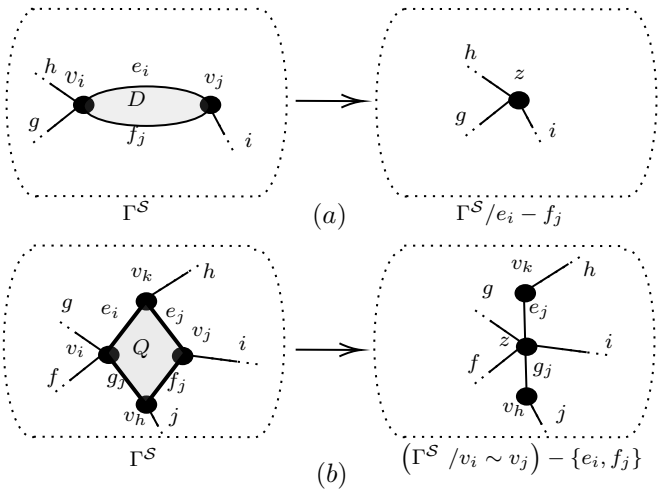

Fig. 3. Two contraction operations.

Proof: It is clear that L_n is bipartite. Therefore, it has no odd cycles. Hence, any embedding of L_n has not odd faces.

■

Leaved dipole rose graphs possess specific counting on their edges. Specifically, such graphs are a special kind of sparse and tight graphs. Let $|V_\Gamma|$ and $|E_\Gamma|$ be the cardinality of the vertex and edge set of Γ, respectively. Let l and k be non-negative integers, with $l \leq k$. A graph $\Gamma = (V, E)$ is called (k, l)- *sparse* if, for every nonempty subgraph Ω of Γ, $|E_\Omega| \leq k|V_\Omega| - l$. Γ is called (k, l)-*tight* if it is (k, l)-sparse and $|E| = k|V| - l$, [17]. Sparse and tight graphs have been the subject of much research and investigations. They have been used in many topics for their counting properties. In graph decomposition, for instance, Nash-William and Tutte [18], [19] stated and proved the well-known tree packing theorem, which states that a graph Γ is the union of k edge-disjoint trees if and only if Γ is (k, k)-tight. An outcome of the tree packing theorem is that a graph Γ has k pairwise edge-disjoint spanning trees if and only if Γ is (k, k)-tight graph, [20].

The *Henneberg type 1* operation is the addition of a vertex of a degree two to a graph. On the other hand, the inverse Henneberg type 1 operation represents deleting a vertex of degree two from a graph, [3]. Figure 4(a) and (b) shows the performing Hanneberg type 1 operation and its inverse on a simple and muligraph, respectively. Shortly, we will see that L_n is $(2, 2)$-tight. Thus, it has 2 pairwise edge-disjoint spanning trees which each one of them is an S_n (star graph).

Proposition 1.2: For $n \geq 2$, L_n can be constructed from a single vertex by n Henneberg operations of type 1.

Proof: Choose a vertex of degree 2 in L_n. Remove this vertex and its two adjacent edges. The resulting graph is L_{n-1}. Therefore, L_n is obtained from L_{n-1} by a Henneberg of type 1 operation. Continuing performing this operation on the graph until no vertex of degree two exist.

■

Lemma 1.3: Henneberg type 1 operation preserves $(2, 2)$-tightness.

Proof: Let $\Gamma = (V, E)$ be a $(2, 2)$-tight and $\Gamma' = (V', E')$ be a graph that is obtained from Γ by performing a Henneberg type 1 operation. Notice that $2|V'| - |E'| =$

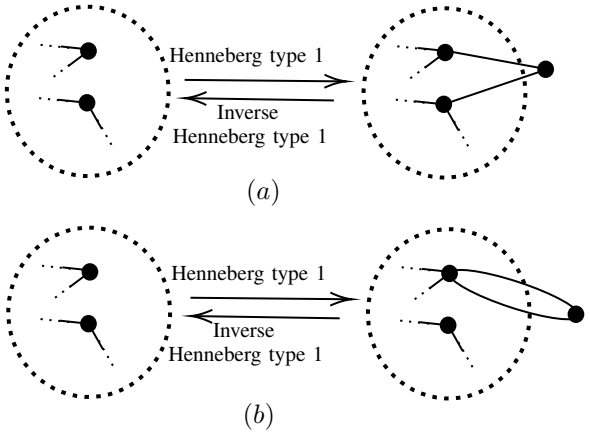

Fig. 4. Henneberg type 1 operations and their inverse.

$2(|V|+1)-(|E|-2)=2|V|-|E|=2$. Now, let Ω be a non-empty subgraph of Γ'. Let v be the vertex that was added by performing the Henneberg type 1 operation. Hence, $2 \leq 2|(V_\Omega \backslash \{v\}) \cup \{v\}| - |(E_\Omega \backslash \{e_1,e_2\}) \cup \{e_1,e_2\}| = 2|V_\Omega \backslash \{v\})| - |(E_\Omega \backslash \{e_1,e_2\}|$ ■

Lemma 1.4: L_n is $(2,2)$-tight.

Proof: This follows from Proposition 1.2 and Lemma 1.3. ■

II. Leaved Dipole Rose Spherical and Cylindrical Graphs

In [21], plane leaved dipole rose graphs were mentioned as self-dual graphs. If a leaved dipole rose graph is embedded in the sphere in such a way that no embedded parallel edges are contained within a digon, then we call such a graph *healthy*.

Lemma 2.1: If L_n^S is healthy, then there are exactly n digons and one $2n$-gonal face.

Proof: By Euler's formula, we have $|V_{L_n^S}| - |E_{L_n^S}| + |F_{L_n^S}| = 2$. But L_n^S is $(2,2)$-tight, so $-|E_{L_n^S}| + 2|F_{L_n^S}| = 2$. But $|E_{L_n^S}| = 2n$, thus $|F_{L_n^S}| = n+1$. Since L_n^S is healthy, it follows that $r_2 = n$ and $r_{2n} = 1$. ■

Lemma 2.2: For $n \geq 2$, L_n^S has at least two digons.

Proof: By Euler's formula, we have $|V_{L_n^S}| - |E_{L_n^S}| + |F_{L_n^S}| = 2$. Since L_n^S is $(2,2)$-tight, so $2-|E_{L_n^S}|+2|F_{L_n^S}| = 4$. But $2|E_{L^S}| = \sum_{i\geq 0} ir_i$, thus we get $-\sum_{i\geq 0} ir_i + 4\sum_{i\geq 0} r_i = 4$. Rearranging the last equation leads to $\sum_{i\geq 0}(i-4)r_i = -4$. Expanding the last equation results in $-4r_0 - 3r_1 - 2r_2 - 3r_3 + r_5 + 2r_6 + \cdots = -4$. It is clear that $r_0 = r_1 = 0$. By Proposition 1.1, we have $r_1 = r_3 = r_5 = r_7 = \cdots = 0$. Thus, $2r_2 = 4 + 2r_6 + 4r_8 + \ldots$. Hence, $r_2 = 2 + 2r_6 + 4r_8 + \ldots$. Consequently, $r_2 \geq 2$. ■

Theorem 2.3: Every n-leaved dipole rose spherical graph (L_n^S) can be reduced to a vertex by n digon contractions towards the core vertex.

Proof: By Lemma 2.2, L_n^S has at least two digons. Pick one of such digons and then contract it. Keep contracting digons until the graph L_n^S be reduced into L_1^S. The latter graph has only two digons. By contracting one of these digons the resulting graph is L_0^S which is just a single vertex. ■

A leaved dipole rose cylindrical graph is minimal if it does not contain a digon or a degenerate quadrilateral.

Theorem 2.4: If L^C is a minimal, then L^C is isomorphic to one of the cylindrical graphs shown in Figure 5

Proof: We see at once that L^C, as a cylindrical graph, either separates the cylinder or does not. We suppose first that L^C does not separate the cylinder. It follows that there is a unique face in L^C which is not cellular. By filling the two boundaries of the cylinder with two open discs, a cellular leaved dipole rose spherical graph L^S is created. Hence, L^S is either a single vertex or it has at least two digons. If L^S has at least two digons then one of these digons must be also a digonal face in L^C which contradicts the minimality of L^C. Now, suppose that L^C separates the cylinder. Clearly, L^C has exactly two noncellular faces. By filling the two noncellular faces with two open discs, a leaved dipole rose spherical graph L^S is created. By Lemma 2.2, there are exactly two digonal faces and these faces are the exceptional faces that are created by the filling process. Therefore, there is no cellular face in L^S other than two digons. In fact, if there are, then all the other faces are quadrilateral which they are also faces of L^C which contradicts the minimality of L^C. Therefore, L^C in this case comprises a pair of parallel edges embedded as a nonseparating cycle in the cylinder, Figure 5(b). ■

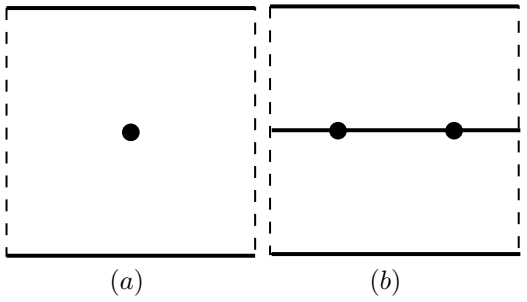

Fig. 5. Leaved dipole rose cylinderical graphs

Theorem 2.5: Every leaved dipole rose cylindrical graph can be contracted into one of the graphs in Figure 5 (a) and (b) by a sequence of digon and quadrilateral contractions.

III. Leaved Dipole Rose Torus Graphs

A leaved dipole rose torus graph is minimal if it does not contain a digonal or a degenerate quadrilateral face. In the following, we give an inductive construction for leaved dipole rose graphs embedded in the torus.

Theorem 3.1: [12] Let G be a (k,l)-tight surface graph and $l \leq k$ and H be a surface subgraph of G. Let F be a face in H. Then,

$$k|V_{H\cup int_G(F)}| - |E_{H\cup int_G(F)}| \leq k|V_H| - |E_H|$$

The following lemma indicates how specific cycles in the torus can be embedded.

Lemma 3.2: Let H be a torus subgraph of a leaved dipole rose torus graph L^T. If H is a separating cycle of length 2 in the torus, then $\widetilde{ext_{L^T}(F)}$ is $(2,2)$-tight where F is a face of H homeomorphic to a punctured torus.

Proof: First of all, we notice that $2|V_{ext_{L^T}(F)}| - |E_{ext_{L^T}(F)}| = 2|V_{\widetilde{ext_{L^T}(F)}}| - |E_{\widetilde{ext_{BIT}(F)}}|$. Now, $2 = 2|V_{L^T}| - |E_{L^T}| = 2|V_{int_{L^T}(F)\cup ext_{L^T}(F)}| -$

$|E_{int_{L^T}(F)\cup ext_{L^T}(F)}|$
$= 2|V_{int_{L^T}(F)}| - |E_{int_{L^T}(F)}| + 2|V_{ext_T(F)}| - |E_{ext_{L^T}(F)}| - 2|V_{\partial F}| + |E_{\partial F}|$
$= 2|V_{int_{L^T}(F)}| - |E_{int_{L^T}(F)}| + 2|V_{ext_{L^T}(F)}| - |E_{ext_{L^T}(F)}| - 2$
So

$$2|V_{int_{L^T}(F)}| - |E_{int_{L^T}(F)}| + 2|V_{ext_{L^T}(F)}| - |E_{ext_{L^T}(F)}| = 4 \quad (1)$$

By Theorem 3.1, $2|V_{H\cup int_{L^T}(F)}| - |E_{H\cup int_{L^T}(F)}| = 2|V_H| - |E_H| + 2|V_{int_{L^T}(F)}| - |E_{int_{L^T}(F)}| - 2|V_{H\cap int_{L^T}(F)}| + |E_{H\cap int_{L^T}(F)}|$
$= 2|V_H| - |E_H| + 2|V_{int_{L^T}(F)}| - |E_{int_{L^T}(F)}| - 2$
$\leq 2|V_H| - |E_H|$
Hence

$$2|V_{int_{L^T}(F)}| - |E_{int_{L^T}(F)}| \leq 2 \quad (2)$$

Now, by the sparsity of L^T we have

$$2|V_{int_{L^T}(F)}| - |E_{int_{L^T}(F)}| \geq 2 \quad (3)$$

Combining 1 with 2 gives

$$2|V_{int_{L^T}(F)}| - |E_{int_{L^T}(F)}| = 2 \quad (4)$$

Substitute 4 in 1 to get $2|V_{ext_{L^T}(F)}| - |E_{ext_{L^T}(F)}| = 2|V_{\widetilde{ext_{L^T}(F)}}| - |E_{\widetilde{ext_{L^T}(F)}}| = 2$. Now, the sparsity of L^T shows that $\widetilde{ext_{L^T}(F)}$ is $(2,2)$-tight. ■

Proposition 3.3: Suppose that L^T is minimal. Then any 2-cycle in L has to be embedded as a nonseparating cycle in L^T.

Proof: On the contrary, suppose that W is a 2-cycle in L which forms a separating cycle H in the torus, where H is the embedding of W in T. Now, consider the spherical graph $\widetilde{ext_{L^T}(F)}$. By Lemma 3.2, $\widetilde{ext_{L^T}(F)}$ is $(2,2)$-tight. By Lemma 2.2, we have at least one digon in $\widetilde{ext_{L^T}(F)}$ that is also a face in L^T which contradicts the minimality of L^T. ■

Theorem 3.4: If L^T is minimal and noncellular, then it is isomorphic to one of the torus graphs in Figure 6(a) and (b).

Proof: Since the surface here is the torus and L^T is connected, then L^T has exactly one face that is not cellular. So L^T might be L^T_0, Figure 6(a). Now, suppose that L^T is not L^T_0. If the noncellular face is a punctured torus then L^T without the punctured face can be considered as a leaved dipole rose spherical graph. By Lemma 2.2, such a graph has two digons and so L^T has a digon which contradicts the minimality of L^T. Therefore, the noncellular face of L^T is an open cylinder. Let α be a loop in the noncellular face, such that α is nonseparating in the torus. If we cut and cap along α, then we obtain L^S. The resulting L^S has two faces that are not faces of L^T. By Lemma 2.2 these two faces must be digons. By applying Lemma 2.2 again, we get that any other faces must be quadrilaterals and these faces are also faces in L^T contradicting the minimality of L^T. Therefore, L^T in this case comprises a pair of parallel edges embedded as nonseparating cycle in T, Figure 6(b). ■

Lemma 3.5: Let L^T be a minimal and cellular. Then, L^T is either a torus graph with only two faces and those faces are hexagons or a torus graph with only one face and that face is an octagon.

Proof: By Euler's formula, we have $|V_{L^T}| - |E_{L^T}| + |F_{L^T}| = 0$. Also, we have $-|E_{L^S}| + 2|F_{L^S}| = 0$. Since $2|E_{L^T}| = \sum_{i\geq 0} ir_i$, the latter equation can be written as $-\sum_{i\geq 0} ir_i + 4\sum_{i\geq 0} r_i = 4$. Rearranging the last equation leads to $\sum_{i\geq 0}(i-4)r_i = 4$. Expanding the last equation results in $-4r_0 - 3r_1 - 2r_2 - r_3 + r_5 + 2r_6 + \cdots = 4$. But L^T is minimal. So, by Proposition 1.1 we get that $2r_6 + 4r_8 = 4$. Thus, $(r_6, r_8) \in \{(2,0),(0,1)\}$. ■

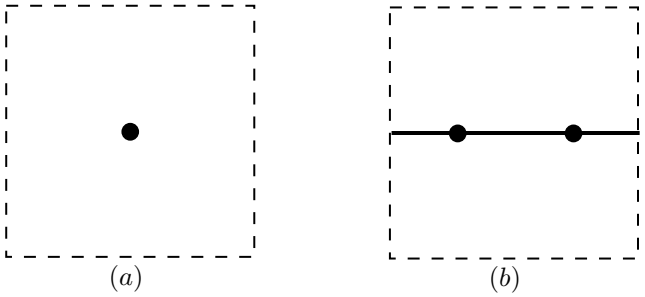

Fig. 6. Leaved dipole rose torus graphs.

Theorem 3.6: If L^T is minimal, then it has at most four vertices.

Proof: If L^T is noncellular, then by Theorem 3.4 we get $1 \leq |V_{L^T}| \leq 2$. Now, suppose L^T is cellular. By the proof of Lemma 3.5, we get $2r_6 + 4r_8 = 4$. But $2|E_{L^T}| = \sum_{i\geq 0} ir_i = 6r_6 + 8r_8$. Hence, $2|E_{L^T}| \leq 3(2r_6 + 4r_8) = 3(4) = 12$. Therefore, $|E_{L^T}| \leq 6$. But L^T is $(2,2)$-tight. So, $|V_{L^T}| = \frac{|E_{L^T}|+2}{2} \leq 4$. ■

To complete the inductive construction of leaved dipole rose graphs that are embedded in the torus, we need to find minimal graphs with three and four vertices. We show in the following that there are only two minimal graphs; one of them with three vertices and the other with four vertices.

Proposition 3.7: If L^T is minimal with three vertices, then it is isomorphic to the torus graph in Figure 7(b).

Proof: By Proposition 3.3, each of the 2-cycles of L_2 should be embedded as a nonseparating cycle. There are only two ways to embed the two 2-cycles as nonseparating cycles; Either they are homotopic to each other or they are not. The former embedding leads to a non-minimal L^T as it is possible to perform quadrilateral contraction. Figure 7(a) shows how the two 2-cycles of 2-leaved dipole rose graph are embedded homotopically to each other. It is clear that the quadrilateral face is contractible. This means that this torus graph is not minimal. Figure 7(b) shows how the two 2-cycles are embedded in such a way that they are not homotopically to each other. The latter embedding yields a minimal L^T. ■

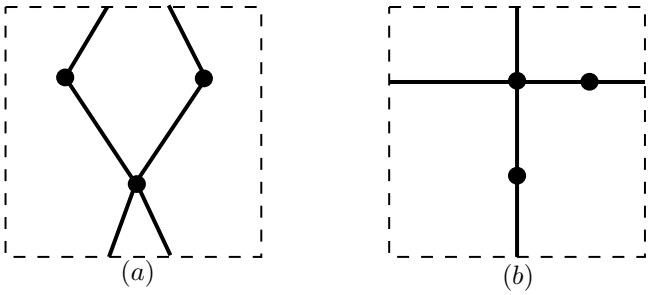

Fig. 7. Two nonhomotopic dipole rose torus graphs.

For the purpose of finding cellular minimal leaved dipole

rose torus graphs with four vertices, we use a useful method of drawing the faces of leaved dipole rose torus with three vertices. This method was proposed in [22]. Figure 8(b) shows a polygon representation of the minimal torus graph in Figure 8(a). We briefly describe the polygon representation method. Let $F_1, F_2, \ldots, F_n$ be the faces of an L^T. Each face F_i is a plane polygon with boundary vertices and edges are labelled by vertices and edges of L^T. Therefore, we can represent L^T by drawing a labelled collection of polygons. We call such a drawing polygon representation. We use this drawing in the proof of Proposition 3.8.

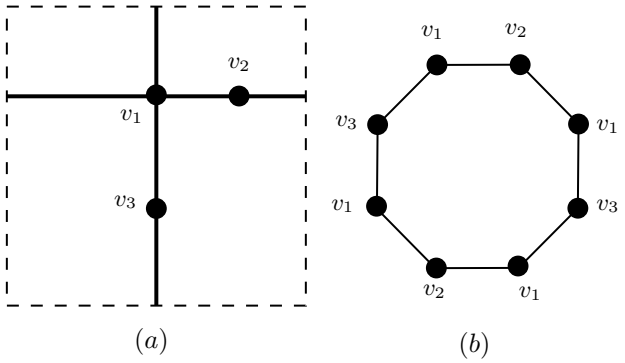

Fig. 8. A leaved dipole rose torus graph with its polygon representation.

Proposition 3.8: If L^T is minimal with four vertices, then it is isomorphic to the torus graph in Figure 9(c).

Proof: We consider L^T with three vertices. Proposition 3.7 asserts that there is only one embedding of a 2-leaved dipole rose graph up to isomorphism. In Figure 8(b), the polygon representation can ease the procedure of embedding the fourth vertex of a 3-leaved dipole rose graph in the torus. Assume the fourth vertex is v_4. Now, to embed this vertex with two incident edges, we can easily realise that there are only two ways to do such an embedding as it is depicted in Figure 9(a) and (b). Therefore, it is clear both of the depicted polygon representations are equivalent to each other. Consequently, the corresponding torus graph of the 3-leaved dipole rose graph is the graph that is isomorphic to the graph in Figure 9(c). ■

Now, by combining the previous results, we obtain the following theorem.

Theorem 3.9: Every cellular leave dipole rose torus graph can be constructed from one of the torus graphs in Figure 8(a) and Figure 9(c) by a sequence of digon or quadrilateral splitting operations.

IV. Conclusion

This work establishes inductive constructions for leaved dipole graphs that are embedded in the sphere, cylinder and torus. For each of these classes of surface graphs, we present an inductive construction which consists of a set of minimal surface graphs and a set of topological inductive operations. For each of such classes of surface graphs, we determined and stated the set of minimal surface graphs.

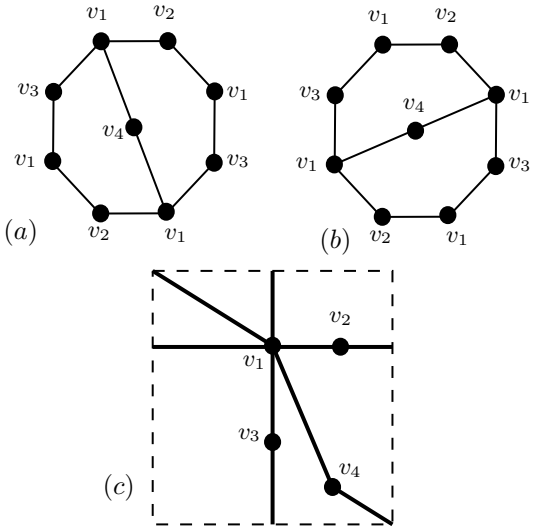

Fig. 9. Two equivalent polygon representations of a torus graph.

References

[1] G. Laman, "On graphs and rigidity of plane skeletal structures", J. Engrg. Math., 4:331340, 1970.

[2] L. Henneberg, "Die graphische statik der starren system"e, Leipzig, 1911.

[3] A. Nixon, J. C. Owen, S. C. Power, "Rigidity of frameworks supported on surfaces", SIAM J. Discrete Math. 26 (4) 17331757, 2012.

[4] E. Androulaki, S. Lambropoulou, I. Economou, J. H. Przytycki, "Inductive construction of 2-connected graphs for calculating the virial coefficients", J. Phys. A: Math. Theor. 43, 2010.

[5] W. Jing-yu , Siqinbate, "Some results of the compact graphs", IAENG International Journal of Applied Mathematics, Vol. 49 Issue 4, 588-594, 2019.

[6] S. A. Lavrenchenko, "Irreducible triangulations of a torus", Ukrain. Geom. Sb.; (30):52-62, ii,1987.

[7] D. Barnette, "Generating the triangulations of the projective plane", J. Combin. Theory Ser. B; 33(3):222-230, 1982.

[8] T. Sulanke, "Note on the irreducible triangulations of the Klein bottle", J. Combin. Theory Ser. B,; 96(6):964-972, 2006.

[9] D. W. Barnette, A. Edelson, "All orientable 2-manifolds have finitely many minimal triangulations", Israel J. Math, 62(1):90-98,1988.

[10] Z. Fekete, T. Jordn,W. Whiteley, "An inductive construction for plane Laman graphs via vertex splitting", in: AlgorithmsESA 2004, Vol. 3221 of Lecture Notes in Comput. Sci., Springer, Berlin, pp. 299310, 2004.

[11] J. Cruickshank, D. Kitson, S. C. Power, "The generic rigidity of triangulated spheres with blocks and holes", J. Combin. Theory Ser. B 122, 550577, 2017.

[12] J. Cruickshank, D. Kitson, S. Power, Q. Shakir, "Topological inductive constructions for tight surface graphs", Graphs and Combinatorics, Graphs and Combinatorics 38, 169 , 1-31, 2022.

[13] B. Mohar, C. Thomassen , "Graphs on surfaces", Johns Hopkins studies in the mathematical sciences. Johns Hopkins University Press, Baltimore, MD, 2001.

[14] D. Archdeacon, "Topological graph theory: a survey", volume 115, pages 5-54. 1996. Surveys in graph theory (San Francisco, CA) 1995. www.math.u-szeged.hu

[15] L.W. Beineke, R. J. Wilson, "Topics in topological graph theory", volume 128 of Encyclopedia of Mathematics and its Applications. Cambridge University Press, Cambridge, 2009.

[16] R. Gelca, "Theta functions and knots", World Scientific Publishing Co. Pte. Ltd., Hackensack, NJ, 2014.

[17] Z. Fekete, L. Szeg o, "A note on [k,l]-sparse graphs", Graph theory in Paris, Trends Math., pages 169-177. Birkhäuser, Basel, 2007.

[18] C. S. J. A. Nash-Williams, "Edge-disjoint spanning trees of finite graphs", J. London Math. Soc., 36:445-450, 1961.

[19] W. T. Tutte, "On the problem of decomposing a graph into n connected factors", J. London Math. Soc., 36:221-230, 1961.

[20] C. S. J. A. Nash-Williams, "Decomposition of finite graphs into forests", J. London Math. Soc., 39:12,1964.

[21] B. Servatius, H. Servatius, "Self-dual maps on the sphere", Discret. Math., 134,139-150, 1994.

[22] Q. Shakir, "Polygon representations of surface graphs", Vietnam Journal of Mathematics (in press)